Transition-State Models and Hydrogen-Isotope Effects

Kinetic isotope effects provide a sensitive test for detailed models of reacting systems.

Ralph E. Weston, Jr.

The branch of physical chemistry encompassed by the term chemical kinetics is a science that operates at many levels of abstraction and refinement. At its least sophisticated level, one may be content to measure the gross rate of formation of two compounds *C* and *D* from compounds *A* and *B*; such measurement may not indicate the many steps and intermediate compounds involved in the reaction. At the other extreme of refinement, one may determine a rate constant or cross section σ_{ijkl} ($\bar{v}_A$, $\bar{v}_B$, $\bar{v}_C$, $\bar{v}_D$) for the process

$$A_i(\bar{v}_A) + B_j(\bar{v}_B) \rightarrow C_k(\bar{v}_C) + D_l(\bar{v}_D) \tag{a}$$

where the subscripts indicate a complete specification of internal quantum states and the $\bar{v}$'s are velocities. Such a detailed cross-section measurement is yet to be made, although molecular-beam experiments are approaching this goal. The prospect of calculating such a cross section a priori appears even further away.

Somewhere between these two extremes is the level at which one attempts to disentangle the mechanism of a complex reaction and to determine the rate constants of individual steps in it. For example, the reaction between hydrogen and chlorine follows the overall equation

$$H_2 + Cl_2 = 2HCl$$

But the individual steps are:

$$Cl_2 \rightleftharpoons 2Cl \tag{b}$$

$$H_2 + Cl \rightleftharpoons HCl + H \tag{c}$$

$$H + Cl_2 \rightleftharpoons HCl + Cl \tag{d}$$

$$H + Cl \rightleftharpoons HCl \tag{e}$$

$$H + H \rightleftharpoons H_2 \tag{f}$$

Suitable experimental techniques permit one to separate step (c) and to determine k_c in the expression

$$d(HCl)/dt = k_c(H_2)(Cl) \tag{1}$$

A reasonable goal for contemporary chemical kinetics is calculation of a rate constant such as k_c, starting from properties of the reactants—in this instance, H_2 and Cl. The machinery for doing this (Fig. 1) is still imperfect and in need of much improvement, but has nevertheless been of great value in sharpening our picture of the reaction process. A major development in kinetic theory about 30 years ago was the transition-state method. I shall now discuss some recent developments in the detailed application of this method, together with specific examples taken from experimental data.

The Activated Complex or Transition State

One of the basic concepts of chemical kinetics was established in 1889 by the great Swedish physical chemist Svante Arrhenius (*1*). From his own experimental work and van't Hoff's, the temperature-dependence of the rate constant for a chemical reaction was known to obey the expression

$$k = A\ e^{-E_a/RT} \tag{2}$$

(In this equation, E_a is now called the activation energy, *T* is the temperature, *R* is the gas constant, and *A* is usually called the preexponential factor.) Arrhenius recognized the parallel between this expression and the analogous one for an equilibrium constant:

$$K = e^{\Delta S/R}\ e^{-\Delta H/RT} \tag{3}$$

where ΔS and ΔH are the entropy and enthalpy changes for the reaction considered. This parallel led him to suggest that chemical reaction involves an equilibrium between normal, unreactive molecules and "active" molecules capable of reacting. Equations 2 and 3 then imply that the active molecules are higher in energy than the normal molecules by an amount E_a. This concept of an activated species has been extremely important to the theoretical development of chemical kinetics. For the specific case of bimolecular reactions such as I shall discuss later, the basic idea was refined and made quantitative in the early 1930's by Pelzer, Wigner, Eyring, Polanyi, and Evans (*2*), the final development being the "absolute rate theory" or "transition-state theory" of Eyring, which had been explicitly formulated by 1935 (*3*). Some major assumptions lurk behind this theory:

1) The potential energy of the reacting system changes in a continuous way from that of the reactants to that of the products; it is at a maximum for some particular configuration of the atoms involved in the reaction. This fact is shown very schematically in Fig. 2, where the energy of the reacting system is plotted against a parameter indicating the progress of the reaction.

2) Systems having this configuration (the activated complex or transition state) are in thermodynamic equilibrium with the reactant molecules.

3) By virtue of the last assumption, one can apply the methods of statistical mechanics to calculate the equilibrium concentration of activated complexes.

This concentration, multiplied by the frequency ($\nu_R{}^{\ddagger}$) with which the activated complex decomposes to form products, is just the rate of reaction. The resulting rate constant is (*4*)

$$k = [Q^{\ddagger}\ e^{-Eo/RT}/Q(\text{reactants})]\ \nu_R{}^{\ddagger} \tag{4}$$

$$= B(T)\ e^{-Eo/RT}\quad . \tag{5}$$

The concentration factor required is given by the expression in brackets, in which the *Q*'s are partition functions and E_o is the energy difference between the activated complex and the ground state of the reactants. If *B(T)* is weakly dependent on *T*, as it usually is, we recognize the Arrhenius expression, with E_o approximately equal to the empirical E_a.

The author is a senior chemist at Brookhaven National Laboratory, Upton, Long Island, New York 11973.

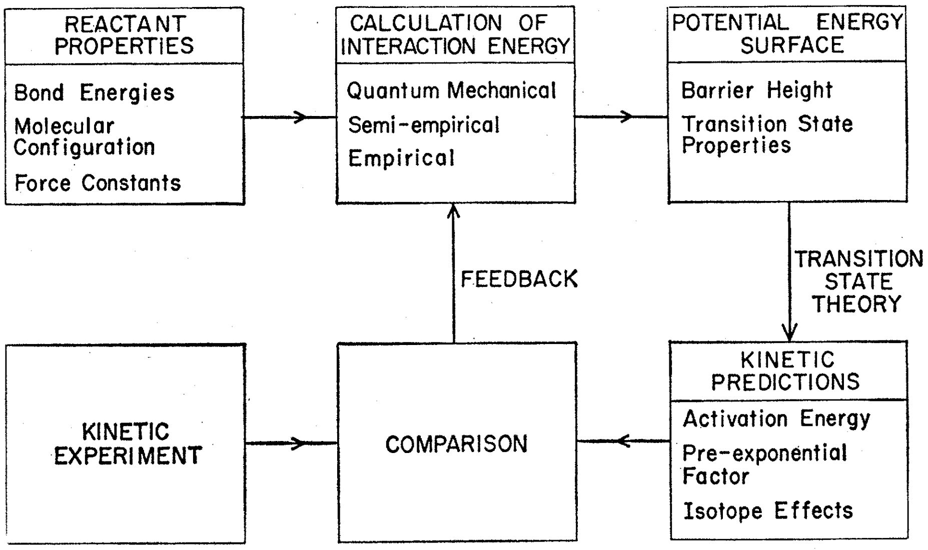

Fig. 1. Schematic flow sheet of the mechanism for making and testing kinetic predictions.

Much energy has been expended in attacking and defending assumptions 1 and 2, above. Here I shall not concern myself with that argument but instead assume the validity of Eq. 4. The remaining problem stems from assumption 3; for, in order to apply the tools of statistical mechanics to the activated complex, one needs to know: (i) the atomic configuration of the transition state, (ii) vibrational frequencies of this species (including the "pseudo vibration" $\nu_R^{\ddagger}$), and (iii) the energy of this state relative to that of reactants.

Potential Energy Surfaces

It is fairly evident that one can obtain the quantities I have just listed if one has detailed knowledge of the potential energy of interaction between all atoms involved in the reaction as a function of interatomic distances. Let us first consider the graphic representation of this point.

For a diatomic molecule AB, the potential energy as a function of internuclear distance can be expressed quite well by a Morse function (Fig. 3):

$$V(R_{AB}) = D_{AB}(e^{-2\beta_{AB}r_{AB}} - 2e^{-\beta_{AB}r_{AB}}) \tag{6}$$

In this expression, D_{AB} is the dissociation energy, r_{AB} is the bond extension from the equilibrium position ($R_{AB} - R_{AB}{}^{o}$), and β_{AB} is an empirical constant that can be evaluated from spectroscopic data.

The next step in complexity, a triatomic molecule ABC, immediately presents a problem: How can we portray the functional dependence of energy on the shape of the molecule (that is, on R_{AB}, R_{BC}, and R_{AC}, or $< ABC$)? Keeping one variable constant (for example, $<ABC$), we can plot lines of constant energy on a contour map, with the other two variables as axes (Fig. 4a). In Fig. 4a the molecule has been constrained to a linear configuration—it might be CO_2, for example. On such a map, the lowest contour represents the most stable molecular configuration: in this case, point *0* at the bottom of an oddly shaped basin. This basin opens out into two higher valleys: the one at upper left corresponding to the system $AB + C$; the similar one at lower right, to $A + BC$. The profile of each valley (that is, the intersection of the energy surface with a plane perpendicular to the paper) is just a two-dimensional energy diagram like that of Fig. 3.

The directions indicated by arrows have particular significance in terms of molecular vibrations (Fig. 4b): the one labeled σ corresponds to the symmetric stretch of the molecule; the one labeled ρ, to the antisymmetric stretch. According to the theory of small vibrations, the potential energy in the immediate vicinity of the equilibrium configuration *0* is

$$2V = F_\sigma(\Delta\sigma)^2 + F_\rho(\Delta\rho)^2 \tag{7}$$

Force constants F_σ and F_ρ can be evaluated from the curvatures of the surface, and finally one can calculate vibrational frequencies by combining these with atomic masses. The bending vibration can be treated in a completely analogous fashion.

Let us now return to our transition-state species and the schematic energy plot of Fig. 2. Evidently, the potential-energy surface for a linear activated complex ABC resembles that of Fig. 4 turned upside down; that is, the basin is replaced by a pass or saddle (Fig. 5). Again note that when R_{BC} is very large we are left with a valley corresponding to unperturbed AB, and vice versa for large values of R_{AB}. The reaction

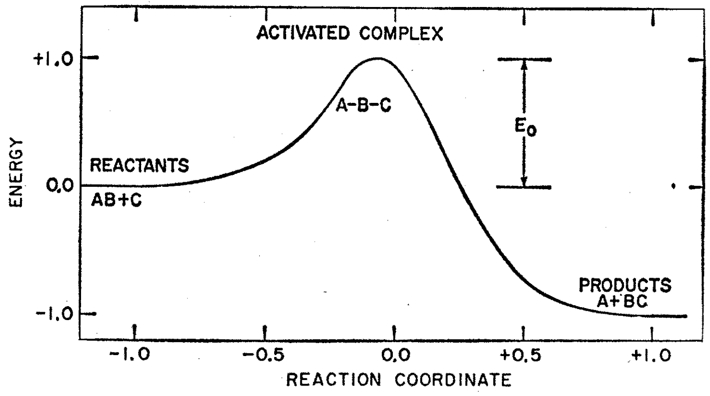

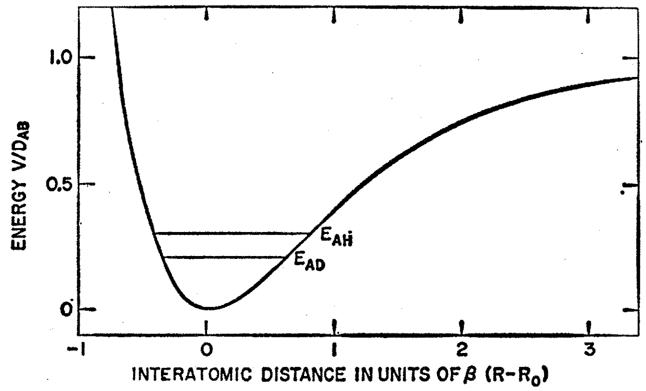

Fig. 2 (left). Potential energy of the reacting system $AB + C$ as a function of a parameter indicating the progress of reaction; E_o is the barrier height or the classical activation energy. Fig. 3 (right). Potential energy of a diatomic molecule AB, as a function of internuclear distance R_{AB}. Also indicated are lowest vibrational levels for the cases $B = \text{H}$ and $B = \text{D}$.

$AB + C \rightarrow A + BC$ can therefore be represented by the dashed line leading from one valley, through the saddle (the transition state), to the other valley; this is the "reaction path" or "reaction coordinate," and plotting of the potential energy as a function of distance along this path yields a diagram such as Fig. 2. The energy plotted in a direction perpendicular to this reaction path gives a diagram similar to Fig. 3, and motion along this path corresponds to the symmetric stretch of the activated complex. For evaluation of the partition function $Q^{\ddagger}$ of Eq. 4, the properties R_{AB}, R_{BC}, and E and the curvatures of the surface are required for the saddle-point configuration.

In principle, extension of these considerations to more complicated systems leads to multidimensional hypersurfaces, always with a transition state stable with respect to motion in all directions but one: the reaction coordinate. At this point I may as well confess that such potential-energy surfaces have rarely been constructed for anything larger than our favorite ABC species. In the discussion to follow I shall generalize slightly by allowing A and C to be polyatomic, but I shall assume that only the potential energy of the three atoms at the reaction center is affected by the process of reaction.

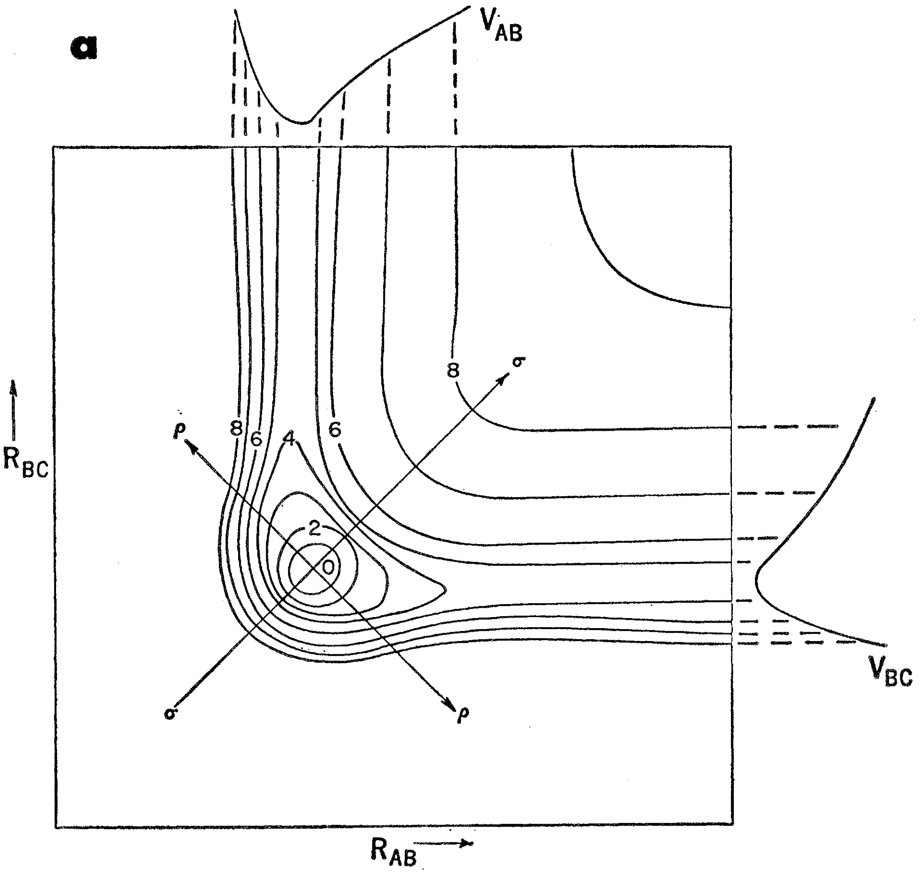

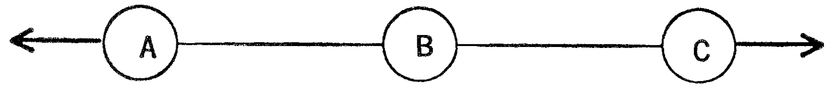

Symmetric stretching vibration (σ)

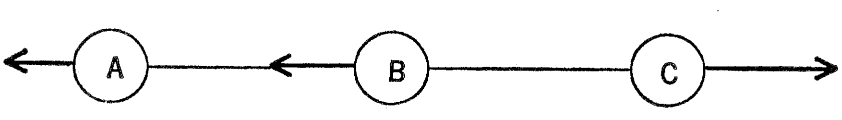

Antisymmetric stretching vibration (ρ)

Fig. 4. (a) Energy contours for a stable, linear molecule ABC as a function of bond lengths R_{AB} and R_{BC}. The Morse-potential curves for the dissociation products AB and BC are also indicated. (b) Stretching vibrations of linear ABC, corresponding to motion along lines $\sigma\sigma$ and $\rho\rho$ of the contour map.

The Calculation of Potential Energies

How can these potential-energy surfaces be constructed? The problem of calculating the energy of a reacting system is no different from that of calculating the energy of a stable molecule. When it comes to details, however, one's initial optimism rapidly evaporates; here are some of the reasons:

1) Quantum chemical calculations of molecular binding energies are accurate within about 1 percent—a few kilocalories per mole, but, according to Eq. 5, a change of 1 kilocalorie per mole in E_o changes the rate constant by almost an order of magnitude at room temperature.

2) The shapes and dimensions of stable molecules are usually known from experiment. This information can be used as input for the energy calculations. But, in order to obtain a potential-energy surface, one must cover a range of configurations corresponding to a large network of points at various values of R_{AB}, R_{BC}, and R_{AC}; the work consumes large quantities of computer time—and of money.

3) For a stable species one can directly compare calculated quantities with those measured experimentally; the comparison is much more indirect in the case of the transition state.

As a result of these restrictions, the only potential-energy surface for which exact quantum mechanical calculations have been made is for the system $H + H_2 \rightarrow H_2 + H$; that is, the *ortho* to *para* conversion of hydrogen. In fact so many different computational methods have been applied to H_3 that it could furnish most of the examples for a course in quantum chemistry. The results (Table 1) are encouraging only in the sense that the most modern and sophisticated procedures are beginning to give activation energies close to those inferred from experiment; even here the extent of the calculated surface is very small—just enough to permit determination of force constants. Extension of this type of calculation from the 3-electron H_3 system to a many-electron case seems a long way off.

Table 1. Binding energy of H_3 (relative to 3H) and activation energy for the reaction of hydrogen atoms with hydrogen molecules; from quantum chemical calculations.

Date	Binding energy (kcal/mole)	V_{act} (kcal/mole)	R_{HH} (Å)
1936	67.1	25.2	0.96
1951	38.5		1.05
1954	72.7	13.8	0.95
1957	60.7		
1958	57.6		.97
1958	72.4	21.0	1.02
1959	68.3		1.00
1959	80.2	15.4	0.94*
1965	91.9	14.3	
1965	104.5	6.2	.91†
	Experimental		
	(100.7)‡	8.7	

* Force constants calculated. † Thirty-five points obtained on surface. ‡ From activation energy and H_2 binding energy.

Impatient with exact theoretical procedures too complex for practical use, chemists have attempted to circumvent this problem by resorting to semiempirical or completely empirical procedures. These methods combine some basis in quantum mechanical theory with empirical observations; in some instances there is a sort of feedback process in which certain kinetic data serve for comparison for the correction of parameters used in the calculation. The predictive value of such a calculation is evidently decreased by this process, but it is still not negligible.

The oldest of the semiempirical methods is a direct descendant of the Heitler-London approach to the calculation of bonding energies of diatomic molecules (*5*). This early method yields as an exact solution for the lowest energy level

$$E_b = (Q_{AB} + \alpha_{AB})/(1 + S^2_{AB}) \qquad (8)$$

The quantities Q, α, and S can be evaluated from the expression for the total energy of the electrons moving in the nuclear field, together with appropriate atomic wave functions. London, somewhat intuitively it appears, extended this method to triatomic molecules and obtained the result (*6*)

$$E_b = Q_{AB} + Q_{BC} + Q_{AC} - 2^{-1/2}[(\alpha_{AB} - \alpha_{BC})^2 + (\alpha_{AB} - \alpha_{AC})^2 + (\alpha_{BC} - \alpha_{AC})^2]^{1/2} \qquad (9)$$

The extremely approximate nature of this expression has been discussed (*7*); it is so severe that the equation must be considered almost purely empirical, and its validity must be indicated by the results obtained from its use.

Even this approximate equation is tedious to evaluate for the many points of a potential-energy surface—or it was so before the days of large digital computers. The first of further assumptions or approximations needed to make it more tractable was introduced by Eyring and Polanyi (*8*) who evaluated the total energy of each diatomic component of the triatomic system from the Morse potential (Eq. 6). This energy was then divided into the contributions Q and α on assumption that the ratio $\rho (\equiv Q/Q + \alpha)$ was independent of internuclear distance. According to the feedback principle already mentioned, one can use ρ as a parameter to be adjusted in some a posteriori manner; usually this has been done by demanding agreement between theoretical and experimental values of the activation energy.

This LEP (London-Eyring-Polanyi) method was applied by Eyring and his co-workers to several reaction systems: $H + H_2$, $H_2 + X$ ($X = F$, Cl, Br, I), $H + CH_4$, and so on. One disquieting property of the potential-energy surfaces for these reactions became apparent when exact quantum mechanical calculations were made for the H_3 system. While the LEP method predicts a basin (corresponding to stability) for the symmetric configuration of this system (Fig. 6), the more rigorous methods did not confirm this, However, they did confirm the prediction that a linear transition state is more stable than a bent one, and henceforth I shall consider only linear configurations.

A modification of the LEP procedure that eliminates the basin was suggested by Sato (*9*, *10*) and has come to be known as the LEPS method. First of all, Sato replaced the factor of $1 + S^2$ that had been dropped when the Heitler-London diatomic expression evolved into the London triatomic formula. The quantity S^2 becomes the adjustable parameter in this approach. The division of total energy into Q and α also follows a different procedure; the important factor here seems to be that the ratio ρ is now dependent on interatomic distance.

Our attempts (*10*, *11*) to evaluate potential-energy surfaces by this method began with very tedious computations, on a desk calculator, for many values of internuclear distances. The corresponding energies were then plotted on a large-scale graph, and, after interpolation between points to rounded values of the energy, contour lines could be drawn. This whole procedure is now

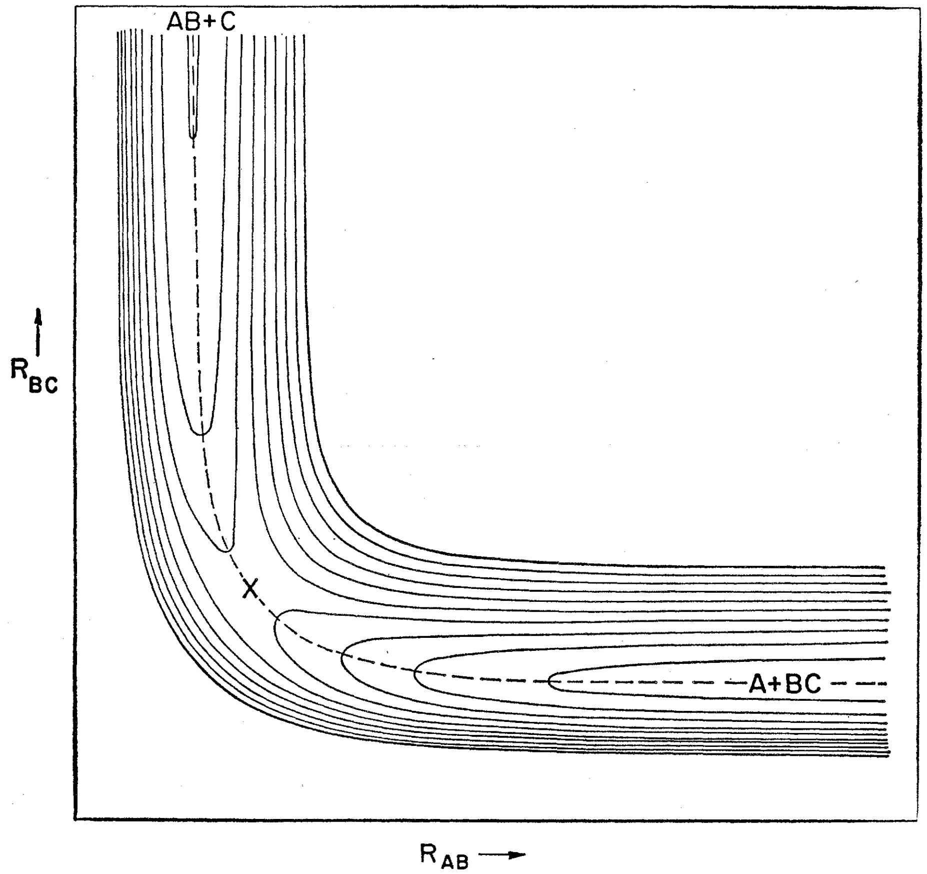

Fig. 5. Energy contours for the reacting system $AB + C \rightarrow A + BC$. The dashed line is the reaction path; the energy profile along this path resembles Fig. 2. The point X represents the transition-state configuration.

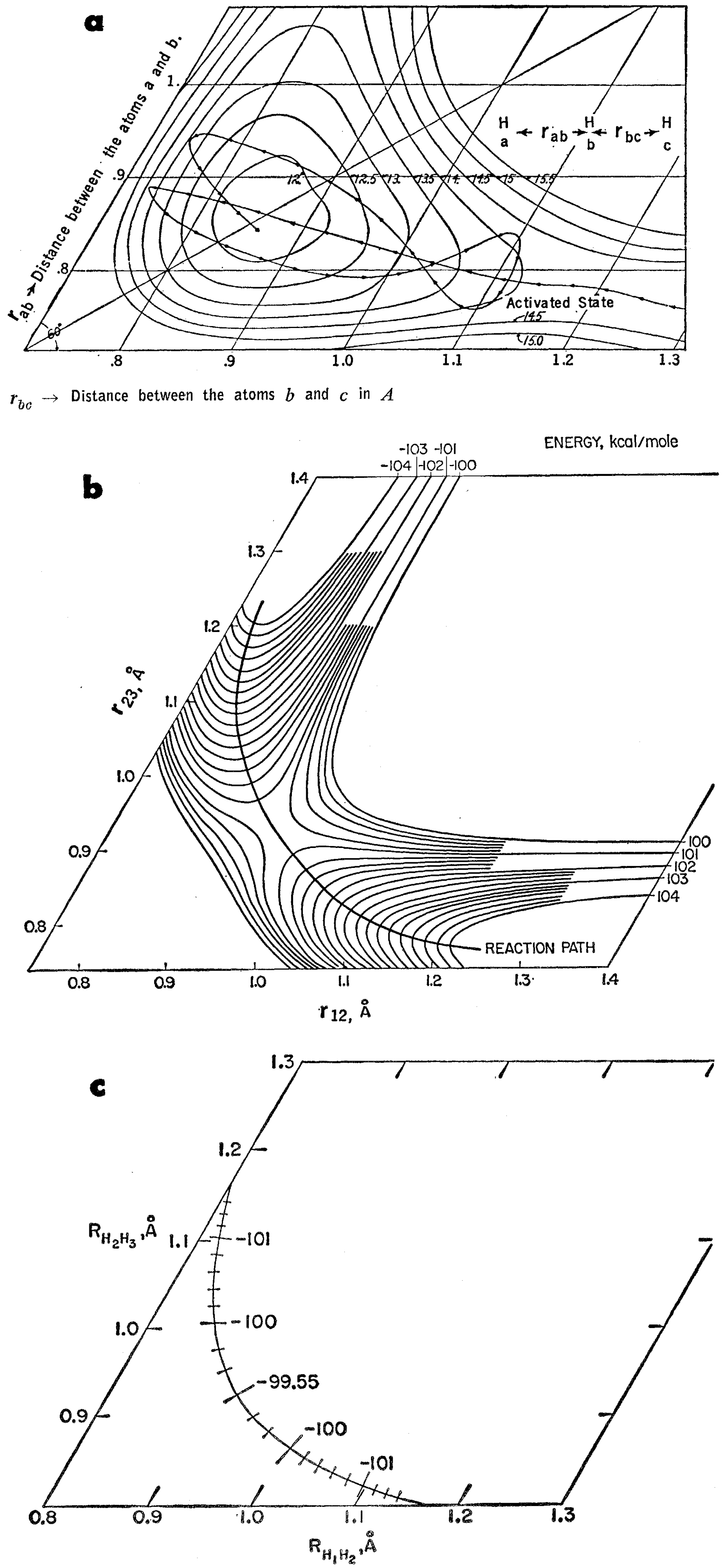

Fig. 6. Potential-energy surface for the reaction $H + H_2$: (a) Semiempirical LEP method [from J. Hirschfelder, H. Eyring, B. Topley, *J. Chem. Phys.* **4**, 170 (1936)]. (b) Semiempirical LEPS method (*10*). (c) Completely empirical BEBO method. Energy "contours" are indicated by short lines perpendicular to the reaction path. The transition state has an energy of − 99.55 kilocalories per mole.

done on a CDC 6600 in something less than a minute of machine time; in fact, Figs. 5 and 11 are from photographs of the cathode-ray-tube display for such a calculation.

A more sophisticated but still semiempirical procedure was used by Porter and Karplus (*12*) to evaluate the potential-energy surface for H_3. Their treatment begins with an expression that is a more general form of the London equation. The dominant diatomic-energy terms in this expression are evaluated from empirical expressions for H_2, and other terms are evaluated either exactly or from simple analytic expressions shown to be good approximations. Their results are in good agreement with those by the LEPS method.

A Completely Empirical Approach

The energy surface for a reacting system would retain its maximum predictive capacity if one could eliminate the necessity for a posteriori adjustment of a parameter used in forming the surface. We have seen already that the chances of doing this rigorously remain tenuous. Suppose we abandon our pretensions to quantum mechanical elegance or rigor and search for a completely empirical method; this has been the approach of Johnston and colleagues (*13*, *14*), and the results have been quite encouraging. Their method of treating atom-transfer reactions involves an assumption that the total bond order (*15*) around the atom being transferred remains constant throughout the reaction process; in addition, empirical relations between bond order and bond length (*16*), bond energy, and vibrational force constants are used. Finally, an expression is derived for the energy of the triatomic system along a reaction path—not for any arbitrary combination of interatomic distances. Thus in this instance the "surface" is really a curve such as that of Fig. 2.

This approach has been labeled the bond energy–bond order or BEBO method. Again for the reaction $H + H_2$, results of this treatment are compared with those by the semiempirical methods in Fig. 6 and Table 2. The agreement between results by this method and by the LEPS method is typical of several systems in which both techniques have been applied.

Table 2. Predicted properties of the H_3 transition state by four methods; md, millidyne.

Property	Boys and Shavitt (*26*)	LEP*	LEPS†	BEBO
E_o ‡(kcal/mole)	15.4	7.6	8.8	9.8
E_a §(kcal/mole)	14.8	8.5	8.0	8.8
R_1 (Å)	0.942	1.354	0.929	0.92
R_2(Å)	.942	0.753	.929	.92
$f(H_1–H_2)$ (md/Å)	.94	4.34	.96	1.32
$f(H_2–H_3)$ (md/Å)	.94	−0.10	.96	1.32
f_{int} (md/Å)	1.31	0.44	1.68	1.89
f_ϕ/R^2 (md/Å)	0.090	.039	0.076	0.048
ν_1 (cm^{-1})	1943	3626	2108	2332
ν_2 (cm^{-1})	950	665	877	695
ν_3 (cm^{-1})	1360*i*	630*i*	1918*i*	1699*i*

* ρ, 0.20. † S^2, 0.1475. ‡ Barrier height. § Activation energy.

Barrier Penetration

Before turning to experimental studies we must explore one more pecularity of the potential-energy barrier separating reactants from products. Picture a roller coaster moving on a track having a vertical profile like that of the curve in Fig. 2; if it starts to move at the left end of the track with total energy equal to or greater than the potential energy it has at the summit, it gets over the hump to the other end of the track; with less initial energy, it slides back and does not cross the barrier. This intuitively obvious result follows from the fact that such things as roller coasters, automobiles, and baseballs obey the laws of classical mechanics. But a much smaller mass, say a hydrogen atom at room temperature (with a de Broglie wavelength of 1 Å), must obey the laws of wave mechanics; because of this wave nature, such a particle can "penetrate" a barrier even when its total energy is less than the barrier height. The probability of such penetration depends on the height and shape of the barrier as well as on the particle mass. We can expect this "tunneling" phenomenon to be of some importance for reactions that involve the transfer of a light atom, especially of one of the isotopes of hydrogen. The result will be an increase in the rate constant as expressed in Eq. 4.

Determination of this correction factor for an arbitrary barrier profile is not simple, even if the shape of the barrier is known exactly. For certain special cases the problem has been solved *(17, 18)*; in particular, a method developed by Eckart (*18*), for an asymmetric barrier of a qualitatively reasonable shape, gives an expression that can be evaluated readily with a digital computer.

I have written here of the barrier as if its shape were a function of only one variable, but the reaction coordinate, even for a triatomic system, is a multivariant quantity. In most instances the response of the kineticist to this situation has been to cross his fingers and continue to treat the problem as if it involved only a separable reaction coordinate. (An example is the profile in Fig. 2, which has been derived from the dotted line on the surface of Fig. 5.) Johnston and Rapp (*19*) have shown how one can carry out a series of calculations for parallel paths on the potential-energy surface; by averaging these results in a suitable way, one hopes to arrive at a better approximation than use of the reaction path alone provides. However, this hope does not appear to be reinforced by the purely quantum calculations of Mortensen and Pitzer (*20*) for the same energy surface. In conclusion, one must retain a lingering doubt whether in reactions in which tunneling is important the theoretical treatment of this phenomenon is adequate.

Predictions from Transition State Models

We have finally reached the point where we are ready to compare experimental results obtained from kinetic studies with predictions from the schematic flow diagram of Fig. 1. The maximum output of this device is (i) the activation energy E_a given by the barrier height E_o, with corrections; (ii) the preexponential factor A, which depends on the detailed partition functions of reactants and transition state; and (iii) relative rate constants for isotopically modified reactants, which depend only on atomic masses and vibrational-force constants of reactants and transition state.

The results of quantum calculations of the activation energy of the $H + H_2$ reaction have already been discussed. At the other extreme of empiricism, the BEBO procedure has been used to predict E_o values for 130 reactions involving transfer of hydrogen atoms between atoms or groups such as Cl, CH_3, OH, and H (*14*); agreement between calculated and experimental values, where the latter are available, is said to be within 2 to 3 kilocalories per mole. Apart from these two extremes of empiricism, it is difficult to make a meaningful test of a model by examination of the activation energy, since this quantity was used to fix a parameter in the semiempirical methods. One could search for a value of the parameter which, when used for many reactions, gave the best average fit; this has not been done.

Preexponential factors have been estimated for various reactions by use of transition-state theory and the semiempirical LEP and LEPS procedures. In general, agreement with experiment is within an order of magnitude; this result is gratifying, but a rigorous test is not imposed on the activated complex models because of the insensitivity of this quantity to details of the model.

Thus one is left with comparison of isotope effects as a test of the semiempirical models. I shall show in the following section that these effects depend on the force constants of reactants and transition state; the latter in turn depend upon the curvature of the potential-energy surface *at the transition-state configuration.* So this is a detailed test of a very small part of the surface. Moreover, these effects are independent of E_o—fortunately, since this datum may have been used already in the choice of some parameter.

There is no reason why one cannot also use the kinetic isotope effect to test surfaces obtained by exact or completely empirical methods; this also has been done.

Theory of Kinetic Isotope Effects

Recent articles in *Science* have discussed isotope effects in chemical equilibria (*21*) and kinetic isotope effects in organic reactions (*22*), so I shall keep this section brief.

The basis for chemical isotope effects on equilibria, together with the results of the transition-state theory outlined above, is all that is necessary for an understanding of isotope effects on reaction rates. It is helpful to consider the equilibrium problem first, and we do this by imagining that our standard reaction $A + BC$ has become reversible. Since the remainder of this article deals with isotopes of hydrogen, let us suppose that the equilibria concern species that differ only by the substitution of a D atom for an H atom:

$$A + B\mathrm{H} \rightleftharpoons A\mathrm{H} + B, \quad K_{\mathrm{H}} \qquad \text{(g)}$$

$$A + B\mathrm{D} \rightleftharpoons A\mathrm{D} + B, \quad K_{\mathrm{D}} \qquad \text{(h)}$$

The two reactions and their equilibrium constants K_{H} and K_{D} can be combined to give

$$B\mathrm{H} + A\mathrm{D} \rightleftharpoons B\mathrm{D} + A\mathrm{H}, \quad K = K_{\mathrm{H}}/K_{\mathrm{D}} \qquad \text{(i)}$$

Reaction (i) is an isotopic-exchange reaction, with an equilibrium constant $K_{\mathrm{H}}/K_{\mathrm{D}}$ that depends on the partition-function ratios $Q_{A\mathrm{H}}Q_{B\mathrm{D}}/Q_{A\mathrm{D}}Q_{B\mathrm{H}}$. It can be shown that such a constant differs from unity only because of quantum effects; in the classical limit there is no discrimination between H and D. What is the molecular source of these quantum effects? The energy of a molecule is a sum of electronic, vibrational, rotational, and translational factors; to a very high degree of approximation, there is no difference between electronic energies of isotopic variants of the same molecule. Rotational and translational motions can be described accurately by classical mechanics and so contribute nothing to the isotope effect. This leaves only molecular vibrations as a source of differences between the equilibrium constants K_{H} and K_{D}, above. Much of this vibrational contribution can be understood by reference to Fig. 3, depicting the potential energy of the AH molecule. According to quantum mechanics, this molecule, vibrating under the influence of its potential energy, has as its lowest energy level $h\nu_{A\mathrm{H}}/2$. The vibrational frequency $\nu_{A\mathrm{H}}$ is determined by the masses of the atoms and the force holding them together. The difference in mass of H and D will produce different vibrational frequencies of AH and AD and a resultant separation of zero-point energies, given by

$$\Delta E_A = h(\nu_{A\mathrm{H}} - \nu_{A\mathrm{D}})/2 \qquad (10)$$

Table 3. Thermochemical properties of halogen atom–hydrogen molecule reactions.

Reaction	ΔH (kcal/mole)	E_a (kcal/mole)	Dissoc. energy of HX (kcal/mole)
H_2 + Cl	1.0	5.5	106.4
H_2 + Br	16.7	17.6	90.3
H_2 + I	32.9	33.4	70.6

A similar relation holds for species BH and BD, but ΔE_B need not be the same as ΔE_A; this point depends on the magnitudes of the vibrational frequencies, and hence on force constants. The energy change in reaction (i) is

$$\Delta E = E_{A\mathrm{H}} + E_{B\mathrm{D}} - (E_{A\mathrm{D}} + E_{B\mathrm{H}}) = \Delta E_A - \Delta E_B \qquad (11)$$

To make this example more explicit, let us assume that ΔE_B is larger than ΔE_A, so that ΔE is negative. The energy of the system can therefore be minimized if the equilibrium moves toward the right in (i), and the equilibrium constant $K_{\mathrm{H}}/\mathrm{K}_{\mathrm{D}}$ exceeds unity; quantitatively this condition is expressed by

$$K_{\mathrm{H}}/K_{\mathrm{D}} = Q_{A\mathrm{H}}Q_{B\mathrm{D}}/Q_{A\mathrm{D}}Q_{B\mathrm{H}} \cong \exp\left[(\Delta E_B - \Delta E_A)/RT\right] \qquad (12)$$

A more accurate expression also takes into account the entropy change in the reaction; specific details are available (*23*). Let me reiterate the main point: the chemical effect of isotopic substitution depends on molecular vibrations. In the case of larger molecules, expressions such as Eqs. 10–12 are replaced by an appropriate summation that takes into account *all* molecular vibrations. The data necessary for evaluation of these expressions are obtained from molecular spectroscopy either directly as vibrational frequencies, or indirectly as force constants used to compute frequencies.

The foregoing discussion needs only slight change to make it applicable to kinetic processes (*24*). For, according to the transition-state hypothesis, an equilibrium is again involved, this time between reactants and the transition state. From Eq. 5 one can compare the rates for $A + B$H and $A + B$D:

$$k_{\mathrm{H}}/k_{\mathrm{D}} = (\nu^{\ddagger}_{A\mathrm{H}B}/\nu^{\ddagger}_{A\mathrm{D}B})(Q^{\ddagger}_{A\mathrm{H}B}/Q^{\ddagger}_{A\mathrm{D}B})(Q_{B\mathrm{D}}/Q_{B\mathrm{H}}) \qquad (13)$$

It is important to note that the term in E_o, an electronic-energy difference, dropped out when one took the ratio $k_{\mathrm{H}}/k_{\mathrm{D}}$. The term containing the $Q^{\ddagger}$'s can be evaluated by exactly the same methods that were just described for an isotope-exchange equilibrium. Again, vibrational frequencies (depending on force constants) provide the basis for the isotope effect, and the magnitude is related to the differences between force constants of the reactants and transition state. However, since one cannot make spectroscopic measurements in the transition state, vibrational frequencies must be obtained from models such as I described earlier. The single important distinction between $Q^{\ddagger}$ of an activated complex and Q of a normal molecule is that one vibrational motion of the latter has been transformed into motion along the reaction coordinate. This motion no longer contributes a difference in zero-point energy, but only the term $\nu^{\ddagger}_{A\mathrm{H}B}/\nu^{\ddagger}_{A\mathrm{D}B}$; again this ratio can be evaluated from the potential surface. If our interest turns toward reactions in which isotopic hydrogen atoms are transferred, it may be necessary also to correct Eq. 13 by a factor that accounts for a mass-dependent difference in "tunneling" ability.

Kinetic Isotope Effects: Experiment and Theory Compared

It is appropriate to consider first the hydrogen atom–hydrogen molecule reaction, since it has always played a key role in the development of chemical kinetics: it is the sole case for which rigorous theoretical calculations have been made, and this particular reaction initiated development of the transition-state theory.

The isotopic modifications of this reaction are

$$\mathrm{H} + para\text{-}\mathrm{H}_2 \rightarrow ortho\text{-}\mathrm{H}_2 + \mathrm{H} \qquad \text{(j)}$$

$$\mathrm{D} + ortho\text{-}\mathrm{D}_2 \rightarrow para\text{-}\mathrm{D}_2 + \mathrm{D} \qquad \text{(k)}$$

$$\mathrm{H} + \mathrm{D}_2 \rightarrow \mathrm{HD} + \mathrm{D} \qquad \text{(l)}$$

$$\mathrm{D} + \mathrm{H}_2 \rightarrow \mathrm{DH} + \mathrm{H} \qquad \text{(m)}$$

Experiments during the 1930's produced the ratio k_k/k_j, but experimental difficulties made it impossible to determine this ratio precisely enough for a useful test of transition-state models. Rates of reactions (j) and (l) have recently been measured by Schulz and LeRoy (*25*), using a fast-flow method of mixing H atoms with H_2 or D_2. Unfortunately, one must still compare rate

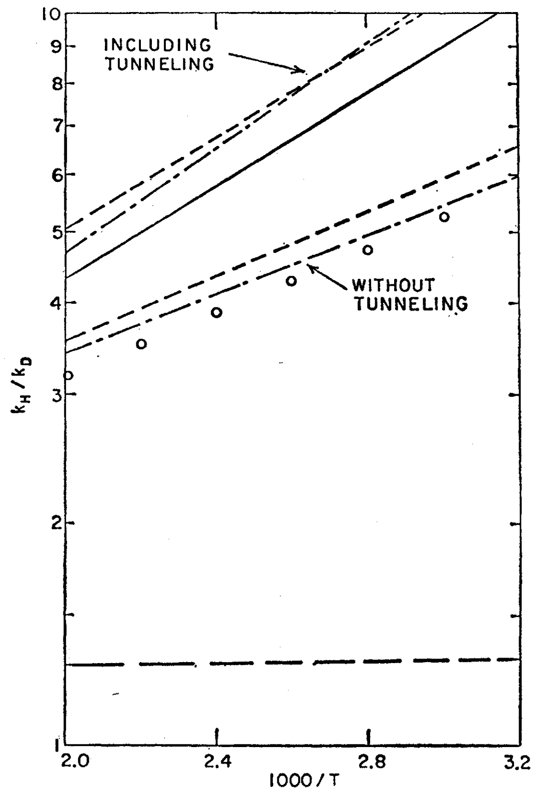

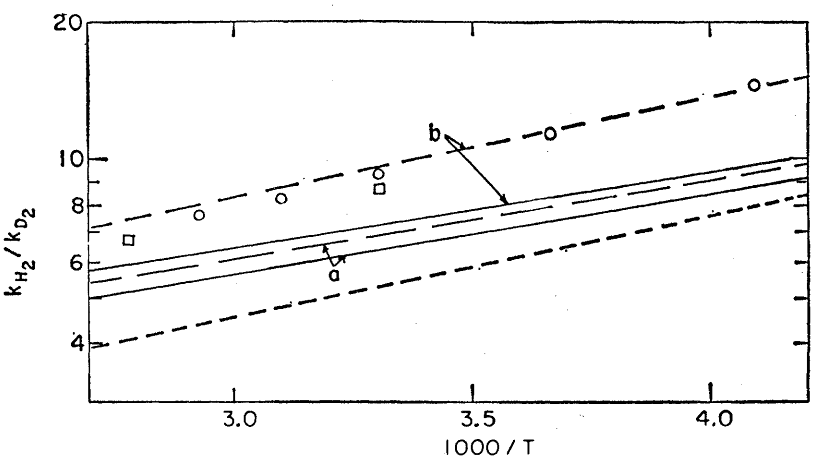

Fig. 7 (left). Ratio of rate constants for the reactions $H + H_2$ and $H + D_2$, as a function of temperature. Circles, experimental values (*25*). Calculated values: — —, LEP (including tunneling); — • —, LEPS; ——, Boys and Shavitt (*26*) (these two surfaces give coincident lines until tunneling is included; - - - -, BEBO.

Fig. 8 (above). Ratios of rate constants for the reactions $Cl + H_2$ and $Cl + D_2$, as a function of temperature. Experimental points: squares (*29*), circles (*30*). Calculated values: ----, LEP (with tunneling); — —, LEPS; ——, BEBO. Labels *a* and *b* indicate that lines lack or include, respectively, a tunneling correction.

constants from separate experiments (in contrast with the method of "isotopic competition" discussed below).

The rate-constant ratio k_H/k_D (or k_j/k_l) is plotted against T^{-1} in Fig. 7, where it is compared with predictions based on various models for the activated complex. The semiempirical LEP method predicts a rate-constant ratio falling woefully short of the measured ratio. This can hardly result from imperfect correction for tunneling; the barrier has a nearly flat top, and the theory is at its best for such cases. Rather, the fault in the LEP surface is that the transition state (reached before passage into the shallow basin) corresponds to a hydrogen molecule only slightly perturbed by the approaching hydrogen atom; thus transition-state force constants differ little from those of the reactant molecule, and from Eq. 13 one may predict a small rate-constant ratio.

The other semiempirical method (LEPS), the completely empirical BEBO procedure, and the quantum calculations of Boys and Shavitt (*26*) give results that are in excellent agreement with each other—in spite of differences in activation energy that they predict (Table 2). Without tunneling corrections, the agreement with experiment is also satisfactory; unfortunately the large tunneling correction required by the predicted thin barriers badly impairs this agreement. At this stage of theoretical imperfection, one does not know whether to attribute this shortcoming to faults in the potential surface or in the procedure used to calculate the tunneling corrections.

The reactions of halogen atoms with hydrogen molecules provide an interesting series having a wide range of activation energies, heats of reaction, and dissociation energies of the resultant HX molecules (Table 3). The mechanism of the hydrogen-chlorine reaction has already been detailed; it proceeds by a chain mechanism, and as a result the rate is extremely sensitive to the presence of impurities affecting the concentration of chlorine atoms. So it is virtually impossible to compare rate constants, for different isotopic species of hydrogen, obtained in "separate but equal" experiments. This difficulty can be circumvented by the isotopic-competition method, which depends on use of a mixture of isotopic species as the reactant; the slow step in the reaction sequence is

$$H_2 + Cl \rightarrow HCl + H$$

If one uses a mixture of H_2 and HD, for example, the two species compete on equal terms for chlorine atoms, according to

$$Cl + \left\{\begin{matrix} H_2 \\ HD \\ DH \end{matrix}\right\} \longrightarrow \left\{\begin{matrix} ClH + H \\ ClH + D \\ ClD + H \end{matrix}\right\} \begin{matrix} k_{H_2} \\ k_{HD} \\ k_{DH} \end{matrix} \qquad (n)$$

The rate-constant ratio $k_{H2}/(k_{HD} + k_{DH})$ can be measured by determination of the change in relative amounts of H_2 and HD left behind as the reaction proceeds; the initial supply of each isotope will be depleted at a different rate.

The transition state for this reaction was the first to be investigated in detail by use of the kinetic isotope effect. Bigeleisen and Wolfsberg (*27*), examining data (*28*) for the H_2-HT system, showed that the LEP model gave unsatisfactory predictions; they also indicated that transition-state force constants could be chosen *ad hoc* to give reasonable agreement between theory and experiment. This isotope effect and effects for other isotopic species were later compared with predictions based on LEPS and BEBO treatments (*11*, *29*, *30*). The predicted rate-constant ratios for $H_2 - D_2$ are compared in Fig. 8; here again one finds that the LEP surface leads to an isotope effect that is too small relative to experiment. However, the cause of this discrepancy is the converse of the effect found in the H_3 activated complex; here the transition state is too nearly like a product molecule, and again there is considerable cancellation between the isotopic differences in reactant and activated complex. The LEPS method, when corrected for a substantial amount of tunneling, leads to predictions that agree well with experiment; predictions by the BEBO procedure are low by 20 to 40 percent.

The experimental work of Persky and Klein (*30*) on this reaction is an isotopic tour de force; I know of no other use of so many isotopic species. Figure 9 compares all their results with predictions by the BEBO method; the agreement (within 20 to 40 percent) is reasonable when one considers that no adjustable parameters were used. Persky and Klein also obtained excellent agreement using a modification of the Sato energy expression; in a sense, this result is disappointing, indicating that probably one cannot relate the isotope effects to a unique potential-energy surface even after use of many isotopic species.

Experimental studies of the bromine atom reaction with hydrogen isotopes parallel those just described, although measurements must be made at higher temperatures because of the greater activation energy (*31*). The theoretically calculated effects are almost uniformly in poor agreement with experiment, no matter which model is used (Fig. 10); this failure originates in the near-coincidence of activation energy (17.6 kilocalories per mole) and heat of reaction (16.7 kilocalories per mole); in forcing the potential-energy surface to yield the correct activation energy, one pushes the transition state into the region corresponding to that of the product (Fig. 11), and the energy difference between transition state and product becomes very small. The same problem arose with the LEP method in the H_2-Cl system. Johnston (*32*) has suggested that in such cases the transition-state method, in general, may be invalid. Since the product molecule must be formed with at least its zero-point energy (3.8 kilocalories per mole), in fact it may be a few kilocalories per mole above the energy barrier; thus a wide region of the potential-energy surface is accessible to it, and the assumption that there is a unique activated-complex configuration at the top of the barrier is unreasonable. On the other hand, the failure to predict correct isotope effects may be related to some fundamental fault of the energy surface itself.

The thermochemical quantities for the $H_2 + I$ reaction are analogous to those of the case of the hydrogen-bromine atoms. However, the isotopic-competition method cannot be used and only the comparison of H_2 with D_2 has been made (*33*). Surprisingly enough, the theoretical isotope effects (from either LEPS or BEBO surfaces) are in much better agreement with experiment than they were for $H_2 + Br$, partly because the experiments are done at higher temperatures; as the temperature dependence in Eq. 12 shows, an error in the predicted zero-point energy differences becomes less serious as the temperature increases.

It is interesting to examine the isotope effects for all three of these reactions collectively (Fig. 12). For each isotopic species, the rate-constant ratios for reactions with the three halogen atoms would be nearly the same if they were measured at the same temperature. The quantum effects on the reactant properties are the same in all three cases (the halogen atom makes no contribution), so the similarity in rate-constant ratios implies that transition-state properties (at least those that regulate isotope effects) are similar in all three reactions. Furthermore, we know that these properties are the vibrational frequencies, which depend on masses and

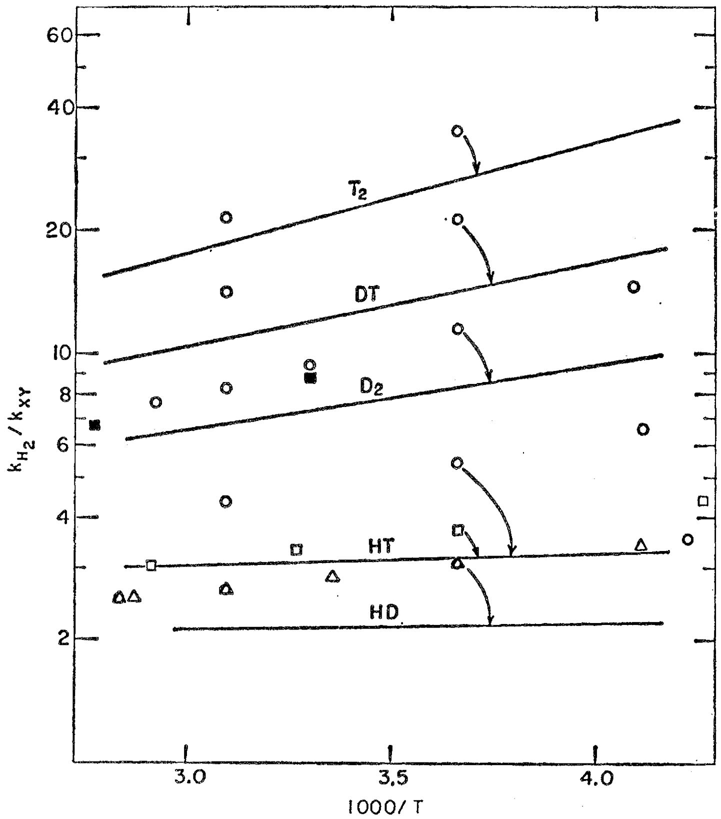

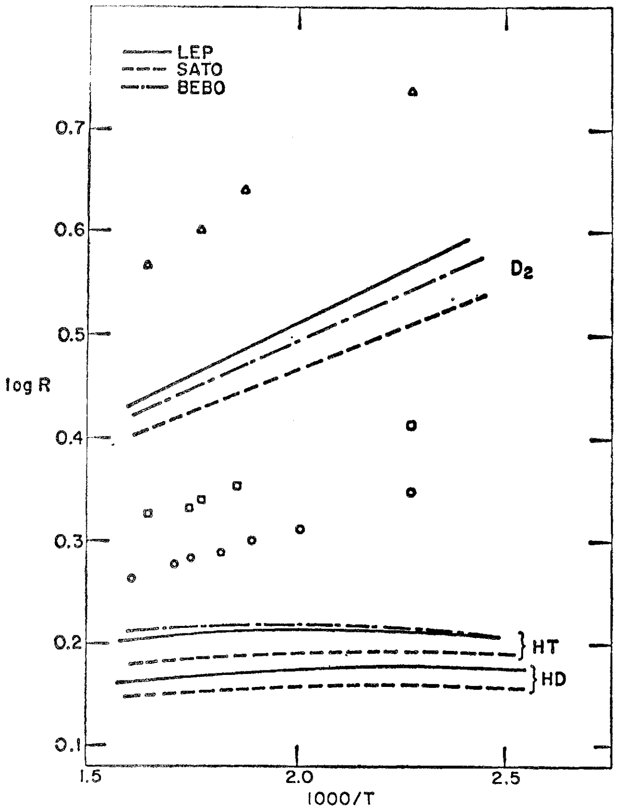

Fig. 9 (left). Rate-constant ratios for reactions of chlorine atoms with various isotopic species of hydrogen. Experimental points: circles (*30*); solid squares (*29*); hollow squares (*HT*) (*28*); triangles (*HD*) (*11*). Solid lines are ratios calculated by the BEBO method, with tunneling corrections included. Fig. 10 (right). Comparison of theoretical and experimental values of log R ($\equiv k_{H_2}/k_{xy}$) for reaction of bromine atoms with isotopic species of hydrogens (*31*). Experimental points: triangles (D_2); squares (*HT*); circles (*HD*). Calculated values: ——, LEP; ---, LEPS; — • —, BEBO. For HD, the LEP and BEBO. lines coincide.

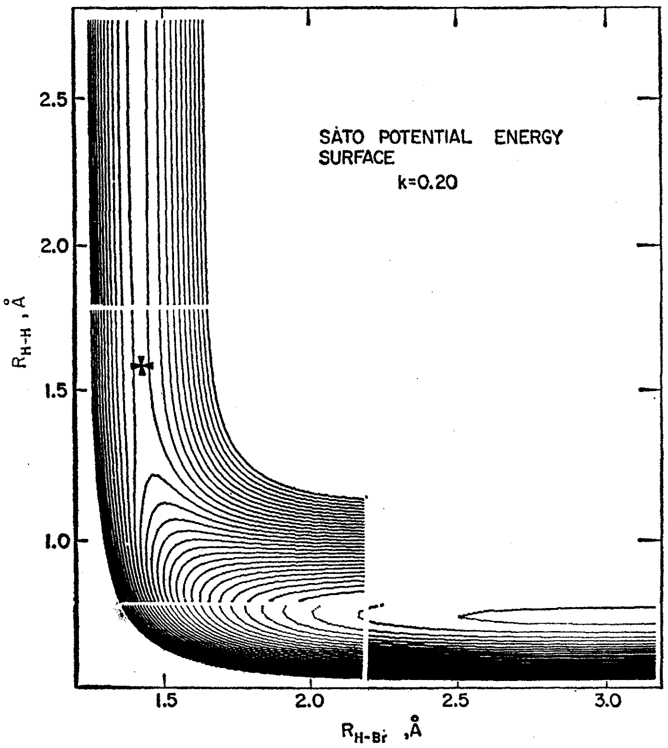

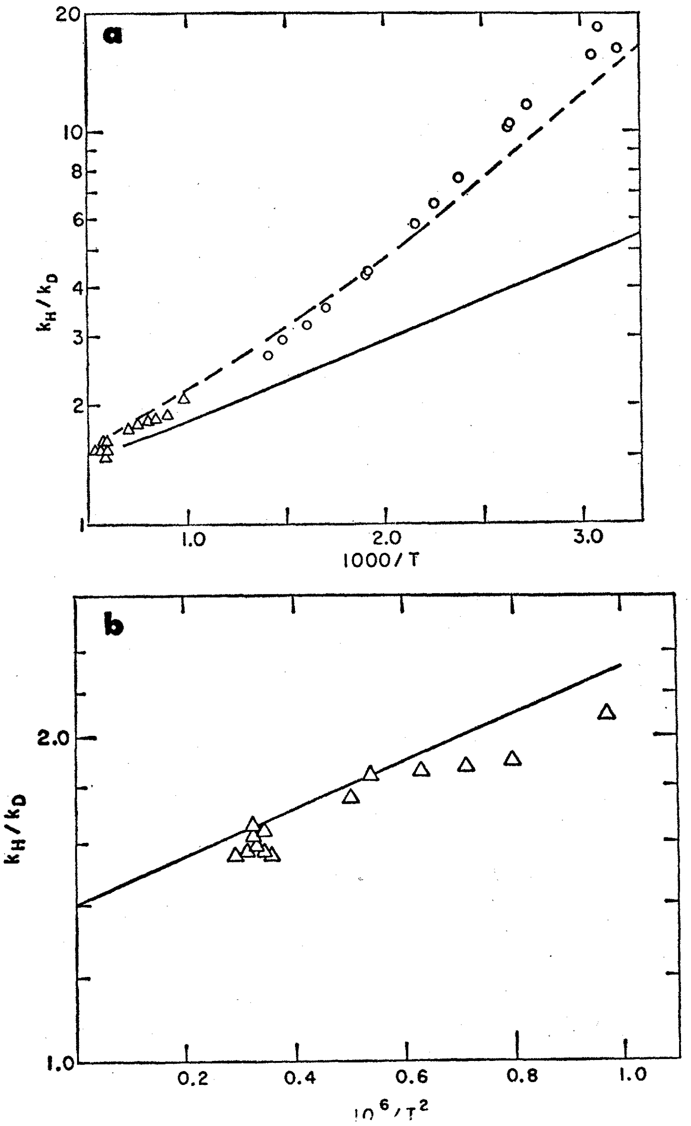

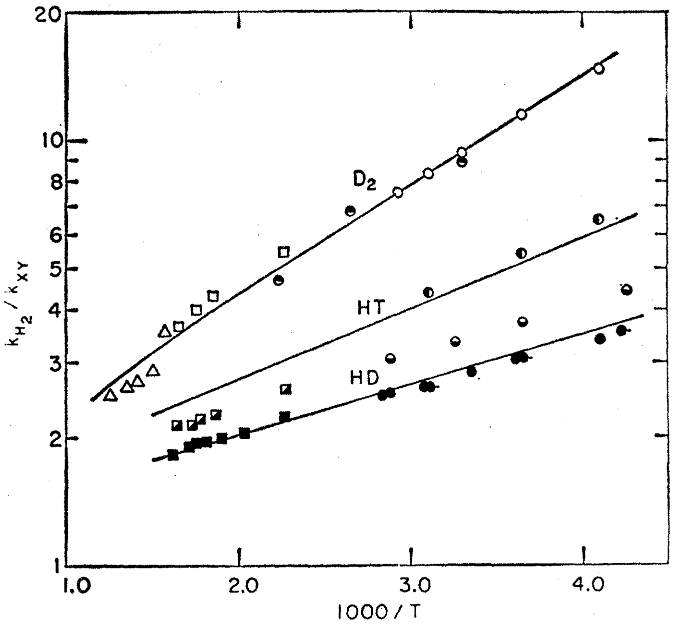

Fig. 11 (top left). Potential energy surface for the H-H-Br activated complex, calculated according to the LEPS method (*31*). The transition-state configuration is indicated by the Maltese cross. The contour interval is 1 kilocalorie per mole, a scale too small to show that the transition state is at a saddle point on the surface. Fig. 12 (bottom left). Hydrogen-isotope effects for reactions of I, Br, and Cl with HD, HT, and D_2. Triangles, I reactions; squares, Br reactions; circles, Cl reactions. The lines are values calculated from an *ad hoc* set of transition-state force constants. Fig. 13 (right). (a) Intramolecular isotope effect for the reaction of CF_3 with CHD_3 (circles) and CH_2D_2 (triangles). Solid line, theoretical values from an LEPS potential-energy surface; dashed line, the same with tunneling correction included; both calculations are for the complete 9-atom model. (b) Enlargement of the high-temperature region of Fig. 13a, with $1/T^2$ as the abscissa. The solid line is the limiting high-temperature value predicted by the model used for Fig. 13a, together with Eq. 15.

force constants; moreover, since the masses in all three transition states are essentially identical (Cl, Br, and I are all infinitely heavy relative to H), the force constants must be the same. Indeed, a purely *ad hoc* choice of force constants does fit these three sets of isotope effects remarkably well (Fig. 12). Unfortunately, this fact seems to be at variance with predictions based on semiempirical or empirical transition-state models, all of which involve some correlation between activated-complex properties and the dissociation energies of the diatomic molecules into which the activated complex can be decomposed.

For the final example I have chosen the reaction between trifluoromethyl radicals and methane:

$$CF_3 + CH_3D \text{ or } CH_2D_2 \rightarrow \left\{ \begin{array}{ll} CF_3H + CH_2D \text{ or } CHD_2, & k_H \\ CF_3D + CH_3 \text{ or } CH_2D, & k_D \end{array} \right\} \quad (o)$$

This demonstrates a particular type of isotopic competition—the *intra*-molecular isotope effect—where both isotopic species are present in the same molecule. The difference in rate constants depends entirely on transition-state properties; in this instance, on differences arising when either an H or a D atom is abstracted from a methane molecule. Relative rates can be obtained simply by mass-spectrometric determination of the CF_3H/CF_3D ratio in the product.

If one makes the simplifying assumption that the important transition-state properties depend only on the 3 atoms at the reaction center, the activated complex can be represented by a very nearly symmetric C. . .H. . .C configuration. Sharp and Johnston (*34*), applying the LEPS method to this problem, have calculated isotope effects on the basis of models of varying complexity, ranging from the triatomic model just described to the complete 9-atom system (*35*). In the latter case, vibrational force constants for the degrees of freedom beyond the C. . .H. . .C framework are incorporated from stable molecules. These various models all give ratios k_H/k_D varying by less than 40 percent. Without tunneling correction, they all predict ratios that are in good agreement with experiment at high temperatures but which diverge from the experimental values increasingly as the temperature drops. This situation is greatly improved by the inclusion of tunneling (Fig. 13a). However, since we have already seen that kinetic isotope effects sometimes can be accounted for by more than one set of force constants, we must question the evidence (Fig. 13a) that tunneling does indeed take place in this reaction.

A unique feature of this experimental work is the very great range in temperature covered (300° to 2000°K). The high-temperature experiments were done in a shock tube (*36*); at low temperature, more conventional photochemical techniques were used (*34*). An unusual test of transition-state theory is made possible by the experiments covering the range 1000° to 2000°K. Wigner and others (*37*) have shown that the quantum partition function at high temperature equals the classical partition function multiplied by a factor

$$1 - (u^2/24), u = hc\nu/kT \qquad (14)$$

Since isotope effects are entirely quantum effects, only these factors will be left in the partition-function ratio of Eq. 13, and we can write for the high-temperature limit of the rate-constant ratio:

$$\ln(k_H/k_D) = \ln(\nu^{\ddagger}{}_{CHC}/\nu^{\ddagger}{}_{CDC}) + [\Sigma_i u_i{}^2(\mathrm{CDC}) - u_i{}^2(\mathrm{CHC})]/24 \qquad (15)$$

This equation indicates that a plot of $\ln(k_H/k_D)$ against $1/T^2$ yields a straight line, with an intercept determined solely by the frequency ratio for the antisymmetric motion of the hydrogen (or deuterium) atom being transferred. The slope of the line depends on all the transition-state frequencies. Both of these line parameters are predicted extremely well by the model used by Johnston *et al.* (Fig. 13b).

Conclusions

The transition-state theory of chemical kinetics, coupled with relatively crude methods of constructing potential-energy surfaces for reacting systems, has great utility in the forecasting of kinetic properties. In particular, it permits prediction of the effect of isotopic substitution on rate constants, and comparison of these predictions with experimental data provides a particularly sensitive test for the combination of potential-energy surface and transition-state theory. More rigorous tests of each of these factors depend on future developments in quantum chemistry, in studies of chemical reactions in molecular beams, and in detailed trajectory calculations of scattering processes.

References and Notes

1. S. Arrhenius, *Z. Physik Chem* **4**, 226 (1889).
2. For references to this early work see S. Glasstone, K. Laidler, H. Eyring, *The Theory of Rate Processes* (McGraw-Hill, New York, 1941).
3. H. Eyring, *J. Chem. Phys.* **3**, 107 (1935).
4. The superscript cross of Lorraine (double dagger), denoting the transition state, causes just as much trouble in oral presentation as it does to the unwary typesetter. One kineticist has overcome the problem by referring to "*Q* tuberculosis" and so on.
5. W. Heitler and F. London, *Z. Physik* **44**, 455 (1927).
6. F. London, *Z. Elektrochem.* **35**, 552 (1929).
7. H. M. James, A. S. Coolidge, R. D. Present, *J. Chem. Phys.* **4**, 187 (1936).
8. H. Eyring and M. Polanyi, *Z. Physik. Chem.* **12B**, 279 (1931).
9. S. Sato, *J. Chem. Phys.* **23**, 592, 2465 (1955); *Bull. Chem. Soc. Japan* **28**, 450 (1950).
10. R. E. Weston, Jr., *J. Chem. Phys.* **31**, 892 (1959).
11. J. Bigeleisen, F. Klein, R. E. Weston, Jr., M. Wolfsberg, *ibid.* **30**, 1340 (1959).
12. R. N. Porter and M. Karplus, *ibid.* **40**, 1105 (1964).
13. H. S. Johnston, *Advan. Chem. Phys.* **3**, 131 (1960).
14. ——— and C. Parr, *J. Amer. Chem. Soc.* **85**, 2544 (1963).
15. Bond order is used here in the simple sense that it is 1 for a C–C bond in ethane; 2, in ethylene; and so on.
16. L. Pauling, *J. Amer. Chem. Soc.* **69**, 542 (1947).
17. R. P. Bell, *Trans. Faraday Soc.* **55**, 1 (1959).
18. C. Eckart, *Phys. Rev.* **35**, 1303 (1930).
19. H. S. Johnston and D. Rapp, *J. Amer. Chem. Soc.* **83**, 1 (1961).
20. E. M. Mortensen and K. S. Pitzer, "The transition state," *Spec. Publ. 16* (Chemical Society, London, 1962), p. 57.
21. J. Bigeleisen, *Science* **147**, 463 (1965).
22. M. J. Goldstein, *ibid.* **154**, 1616 (1966).
23. J. Bigeleisen and M. G. Mayer, *J. Chem. Phys.* **15**, 261 (1947).
24. J. Bigeleisen, *ibid.* **17**, 675 (1949); ——— and M. Wolfsberg, *Advan. Chem. Phys.* **1**, 16 (1958).
25. W. R. Schulz and D. J. LeRoy, *J. Chem. Phys.* **42**, 3869 (1965); *Can. J. Chem.* **42**, 2480 (1964).
26. S. F. Boys and I. Shavitt, *Tech. Rept. WIS-AF-13* (1959); I. Shavitt, *J. Chem. Phys.* **31**, 1359 (1959).
27. J. Bigeleisen and M. Wolfsberg, *J. Chem. Phys.* **23**, 1535 (1955).
28. W. M. Jones, *ibid.* **19**, 78 (1951).
29. G. Chiltz *et al.*, *ibid.* **38**, 1053 (1963).
30. A. Persky and F. S. Klein, *ibid.* **44**, 3617 (1966).
31. R. B. Timmons and R. E. Weston, Jr., *ibid.* **41**, 1654 (1964).
32. H. S. Johnston, *Gas Phase Reaction Rate Theory* (Ronald Press, New York, 1966).
33. J. H. Sullivan, *J. Chem. Phys.* **39**, 3001 (1963).
34. T. E. Sharp and H. S. Johnston, *ibid.* **37**, 1541 (1962).
35. For criticism of these comparisons, see M. J. Stern and M. Wolfsberg, *ibid.* **45**, 4105 (1966).
36. H. S. Johnston and E. Tschuikow-Roux, *ibid.* **36**, 463 (1962).
37. E. Wigner, *Phys. Rev.* **40**, 749 (1932); K. F. Herzfeld and E. Teller, *ibid.* **54**, 912 (1938); J. E. Mayer and W. Band, *J. Chem. Phys.* **15**, 141 (1947).
38. Article prepared under the auspices of the AEC.